High pressure limiting forms of the zero-temperature equations of state of Ta and Pu from relativistic Thomas-Fermi theory

F. E. Leys,[1] N. H. March,[1,2] and D. Lamoen[1]
[1]*Physics Department, Antwerp University, Groenenborgerlaan 171, B-2020 Antwerpen, Belgium*
[2]*Oxford University, Oxford, England*

(Received 3 May 2002; revised manuscript received 25 October 2002; published 28 February 2003)

There is considerable current interest in the equations of state (EOS) of the two heavy metals, tantalum and plutonium. For the former, Boettger [Phys. Rev. B **64**, 035103 (2001)] has recently carried out calculations based on the Dirac relativistic wave equation. Our purpose here is different, namely, it is to work with the simplest form of relativistic density-functional theory which is the relativistic Thomas-Fermi (TF) method. The predictions of this approach should come into their own at sufficiently high pressures (we work throughout at $T=0$) and direct contact has been made, for Ta, with the (lower-pressure) predictions of Boettger's study. Similar results for the high-pressure limiting form of the $T=0$ EOS for Pu are presented. Because the relativistic TF method is purely ''local density'' in character, the results on Ta and Pu are preceded by a full study of the relativistic homogeneous electron gas, including the relativistic exchange contribution to its EOS. An important finding there is that in the high-density limit the relativistic exchange contribution to the pressure becomes proportional to the kinetic contribution, the proportionality constant being linear in the fine-structure constant.

DOI: 10.1103/PhysRevB.67.064109 PACS number(s): 71.15.Rf

I. INTRODUCTION

There is currently considerable interest in the equations of state (EOS) of the two heavy metals Ta and Pu. For the former of these materials, Boettger[1] has recently reported calculations (at $T=0$, which is the case also considered throughout the present paper) based on the Dirac relativistic wave equation. Our purpose in the present work is different in that we shall use the simplest relativistic density-functional theory (DFT), namely, the relativistic Thomas-Fermi (TF) method, originating from the study of Vallarta and Rosen (VR).[2] Boettger's study will, however, prove invaluable since the TF method comes into its own in the present context only as a limiting form of the $(T=0)$ EOS at exceedingly high pressures. It is therefore satisfying that Boettger's wave-function calculations are found to join relatively smoothly with our limiting high-pressure results for the case of Ta. [A very short preliminary report[3] of these numerical results was given by one of us (F.E.L.) at the High Pressure Conference in Santander in 2001.]

Important background for the present study goes back to the investigations of Slater and Krutter[4] and Feynman *et al.*[5] These authors used the nonrelativistic TF method,[6,7] and a number of features of the present study is common to their work. For example, in both approaches, the detailed crystal lattice is not considered, but rather a spherical (Wigner-Seitz) cellular approximation[8] is adopted. This is clearly best for high-symmetry lattices such as face-centered cubic, and becomes less accurate for lower coordination numbers. However, it became clear from the work of Sönderlind *et al.*[9] that one can expect all elements, even those exhibiting very low-symmetry structures at normal conditions such as Pu, to eventually transform to higher-symmetry structures as the bandwidth of the bonding electrons increases with pressure. Secondly, it was proved by Slater and Krutter that in the original TF method the $(T=0)$ pressure-volume relation was determined entirely by the boundary electron number density, $\rho(R)$, say, where R denotes the radius of the Wigner-Seitz (WS) sphere. And indeed, as one would intuitively then expect, since the pressure in this model is due to the electrons bombarding the surface of the WS sphere, the pressure is given by the usual uniform electron-gas relation

$$p=\text{const}\times\{\rho(R)\}^{5/3}. \tag{1}$$

Of course, $\rho(R)$ must be determined self-consistently, with the appropriate boundary condition at $r=R$ being

$$\left.\frac{\partial\rho(r)}{\partial r}\right|_{r=R}=0, \tag{2}$$

which reflects, in the spherical cell approximation, the ''periodicity'' requirement that the normal gradient of the electron density across the WS polyhedron of the appropriate lattice be zero everywhere. Equation (2) is also, of course, a basic boundary condition in relativistic TF theory. But Eq. (1) must naturally be modified to take account of the nonzero value of the fine-structure constant $\alpha=e^2/\hbar c$. Furthermore, Eq. (1) as used by Slater and Krutter,[4] while a rigorous consequence of the original TF method, must also be corrected in more quantitative work, for electron exchange plus correlation interactions.

At the outset of the present study, we emphasize that we shall retain within the relativistic TF framework, the intuitive reasoning stressed above in relation to the Slater-Krutter investigation, that the boundary density $\rho(R)$ is all important in determining the relativistic TF equation of state. Then all that one must do is to use a careful approximation with the equation of state of a relativistic homogeneous electron gas (RHEG), before replacing the constant density, ρ_0, say, in that theory for the pressure p, by the boundary density $\rho(R)$.

It is fortunate for our present purposes that the work of MacDonald and Vosko[10] on electron exchange within a relativistic framework was already available to us. Therefore, the natural starting point for the present investigations was to make a careful numerical study of the EOS of the RHEG.

Thus the outline of the paper is then as follows. In Sec. II immediately below, such EOS data for the RHEG are first presented. This is followed in Sec. III by an account of the generalization of the Slater-Krutter approach that we have adopted to treat the self-consistent relativistic TF method. Here, as known from earlier workers,[11] it is essential to avoid the point-charge nucleus naturally adopted by Slater and Krutter. This is because, though the electron density $\rho(r)$ is infinite at such a point nucleus, one still can impose within the nonrelativistic TF theory the normalization condition

$$\int \rho(\mathbf{r})d\mathbf{r}=Z, \tag{3}$$

where Z is the atomic number. But in the Vallarta-Rosen theory with a point nucleus, the divergence is too strong to allow the normalization condition (3) to be imposed. In Sec. IV a full discussion of the numerical results obtained in this work is presented. An important aspect of Sec. IV is to examine fully how the boundary density $\rho(R)$ is influenced by the finite size of the nucleus. A check on our procedure will then be to ''switch off'' the fine-structure constant α within VR theory in the presence of a finite-size nucleus and hence compare the boundary density we obtain with the nonrelativistic Slater-Krutter values. Furthermore, detailed results for both the $T=0$ EOS for Ta and Pu, which are, as already emphasized above, to be regarded as limiting forms valid at high pressure, are presented. Contact is then also established for Ta with the results of Boettger obtained using the Dirac relativistic wave equation. For both elements, comparison will also be made with predictions from analytic EOS. Section V constitutes a summary, with some possible directions presented for future work in this area. In an Appendix, some thermodynamic considerations are set out, with applications summarized to both the nonrelativistic and relativistic inhomogeneous electron gases.

II. EOS OF A RELATIVISTIC HOMOGENEOUS ELECTRON GAS

A. Analytic form of the EOS

The chemical potential μ_α of the electron gas is given by

$$\mu_\alpha=\frac{\partial t_\alpha}{\partial\rho}+\frac{\partial\varepsilon_{xc\alpha}}{\partial\rho} \tag{4}$$

with t_α and $\varepsilon_{xc\alpha}$, respectively, the kinetic and exchange-correlation contributions to the total-energy density. The index α denotes the fact that we consider the general case where the fine-structure constant α is allowed to be different from zero. Alternatively, since the chemical potential is the Gibbs free energy per particle, one has immediately at $T=0$ the result

$$\mu_\alpha=\frac{E_\alpha}{N}+\frac{p_\alpha v}{N}, \tag{5}$$

where N and v are, respectively, the total number of fermions and the total volume they occupy. Combining Eqs. (4) and (5) one reaches the desired form for the pressure p_α,

$$p_\alpha=\left[\rho\frac{\partial t_\alpha}{\partial\rho}-t_\alpha\right]+\left[\rho\frac{\partial\varepsilon_{xc\alpha}}{\partial\rho}-\varepsilon_{xc\alpha}\right]. \tag{6}$$

Of course, since Eq. (6) is a thermodynamic result, it is immediately applicable to both the relativistic and nonrelativistic cases.

As an immediate check of Eq. (6) we insert the well-known[12] nonrelativistic results for the kinetic-energy density, say, t, and the exchange energy density, say, ε_x,

$$t=c_k\rho_0^{5/3}$$

with

$$c_k=\frac{3h^2}{10m}\left(\frac{3}{8\pi}\right)^{2/3} \tag{7}$$

and

$$\varepsilon_x=-c_x\rho_0^{4/3}$$

with

$$c_x=\frac{3}{4}\left(\frac{3}{\pi}\right)^{1/3}e^2 \tag{8}$$

and immediately obtain the nonrelativistic EOS in the exchange-only approximation

$$p_{\alpha=0}=\frac{2}{3}c_k\rho_0^{5/3}-\frac{1}{3}c_x\rho_0^{4/3} \tag{9}$$

in correspondence with the nonrelativistic virial theorem

$$3p_{\alpha=0}v=2T_{\alpha=0}+V_{\alpha=0}, \tag{10}$$

where $T_{\alpha=0}$ and $V_{\alpha=0}$ denote the total kinetic and potential energies, respectively. The total nonrelativistic pressure and its two constituents are plotted in Fig. 1. Some aspects of a relativistic generalization of this virial theorem, within the approximate theory considered here, are also discussed in the Appendix.

B. Expressions for relativistic energy densities

1. Kinetic

In the general case, we have that

$$\frac{\partial t_\alpha}{\partial n}=\sqrt{c^2p_f^2+m_0^2c^4}-m_0c^2, \tag{11}$$

where the Fermi momentum p_f is related to the uniform electron density ρ_0 by the usual phase-space result

$$\rho_0=\frac{8\pi}{3h^3}p_f^3. \tag{12}$$

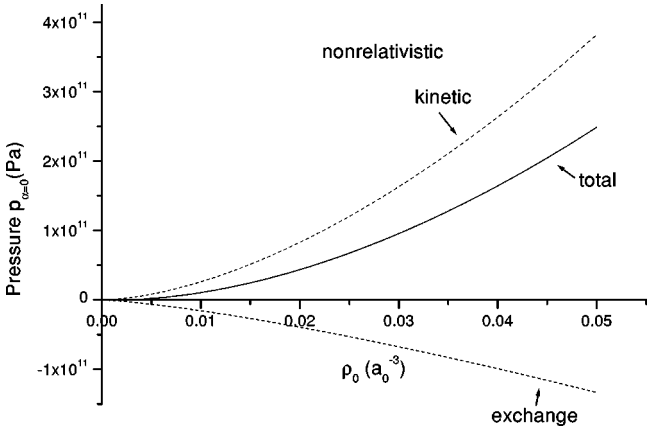

FIG. 1. Pressure of a nonrelativistic uniform electron gas in the exchange-only approximation versus electron density. Kinetic and exchange contributions are shown separately from the total pressure.

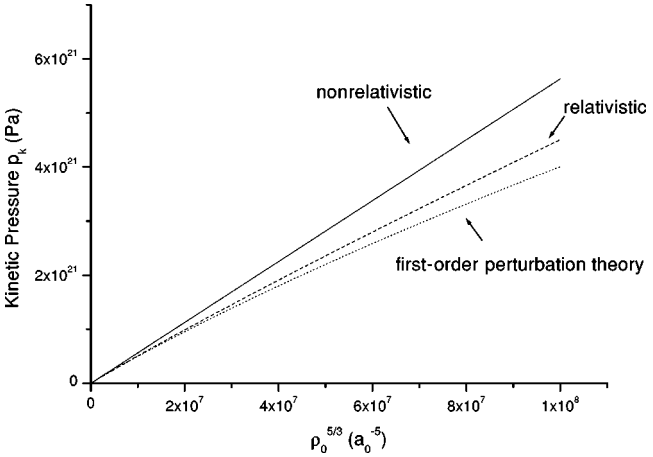

FIG. 2. Nonrelativistic and relativistic kinetic pressures versus $\rho_0^{5/3}$. The result from first-order perturbation theory is also shown.

In writing Eq. (11) one has replaced the nonrelativistic kinetic energy at the Fermi momentum, namely, $p_f^2/2m_0$, by the special relativity form of the kinetic energy, the rest mass energy m_0c^2 being subtracted in the usual way. This procedure can, in fact, be traced back to Vallarta and Rosen.[2] Following Baltin and March,[13] Eq. (11), combined with Eq. (12), can be integrated to yield t_α in the form

$$t_\alpha = a\left\{\beta\left(\frac{1}{2}+\beta^2\right)(1+\beta^2)^{1/2} - \frac{4}{3}\beta^3 - \frac{1}{2}\ln[\beta+(1+\beta^2)^{1/2}]\right\} \tag{13}$$

with the basic dimensionless variable given by $\beta = b\rho_0^{1/3}$ and the constants

$$a = \left(\frac{1}{4\pi^2}\right)\left(\frac{m_0c}{\hbar}\right)^3 m_0c^2, \quad b = (3\pi^2)^{1/3}\left(\frac{\hbar}{m_0c}\right). \tag{14}$$

2. Exchange correlation

The expression for the relativistic exchange energy density $\varepsilon_{x\alpha}$ obtained by MacDonald and Vosko[10] is given in terms of β by

$$\epsilon_{x\alpha} = \varepsilon_x F(\beta) = -c_x\rho_0^{4/3}\left[1 - \frac{3\{\beta(1+\beta^2)^{1/2} - \ln[\beta+(1+\beta^2)^{1/2}]\}^2}{2\beta^4}\right] \tag{15}$$

with, of course,

$$F(\beta) \underset{\alpha\to 0}{\longrightarrow} 1. \tag{16}$$

The importance of correlation effects for the RHEG was thoroughly studied by Kenny *et al.*[14] using quantum Monte Carlo simulations. They concluded, however, that correlation effects become negligible compared to exchange effects already at compression values much smaller than the range of densities of interest here. We will not, therefore, include a study of the relativistic correlation contribution to the pressure here.

C. Discussion of the results

1. Kinetic pressure p_k

Figure 2 compares the kinetic contribution to the pressure, say, p_k, both for the relativistic and nonrelativistic cases. In terms of the variable $\rho_0^{5/3}$ the nonrelativistic result is presented with the straight line, and the effect of relativity is seen to reduce p_k.

For comparison we have also examined limiting forms for the relativistic correction to the kinetic pressure. Starting from the expression for the so-called mass-velocity term[15] H_{mv}, which corrects the nonrelativistic kinetic-energy operator to order α^2,

$$H_{mv} = -\frac{\hat{p}^4}{8m_0^3c^2}, \tag{17}$$

we immediately obtain, for a noninteracting unpolarized homogeneous electron gas, a correction to the kinetic pressure given in first-order perturbation theory by

$$\Delta p_{k\alpha} = -A\rho_0^{7/3} \tag{18}$$

with the constant A given by

$$A = \frac{\hbar^4}{m_0^3c^2}\frac{1}{42\pi^2}(3\pi^2)^{7/3}. \tag{19}$$

This result is also plotted in Fig. 2 in terms of $\rho_0^{5/3}$. The first-order correction is seen to eventually lead to an overestimate of the correction due to relativity that is of the order of the correction itself. In the ultrarelativistic limit $p_fc \gg m_0c^2$ the relativistic kinetic-energy density reduces to

$$t_\alpha \underset{\rho_0\to\infty}{=} \frac{3}{4}(3\pi^2)^{1/3}\hbar c\rho_0^{4/3}, \tag{20}$$

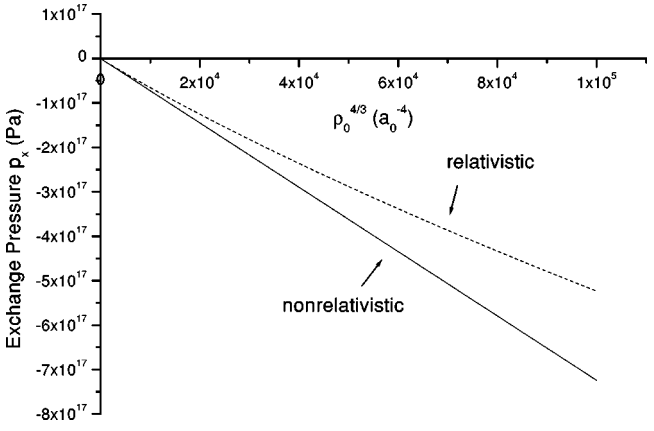

FIG. 3. Nonrelativistic and relativistic exchange pressures versus $\rho_0^{4/3}$.

which immediately yields a pressure from Eq. (6) given by

$$p_{k\alpha} \underset{\rho_0\to\infty}{=} \frac{1}{4}(3\pi^2)^{1/3}\hbar c\rho_0^{4/3}, \tag{21}$$

a result already obtained by, e.g., Landau and Lifshitz.[16]

2. Exchange pressure p_x

Figure 3 compares the exchange contribution to the pressure, say, p_x, both for the relativistic and nonrelativistic cases. In terms of the variable $\rho_0^{4/3}$ the nonrelativistic result is presented by the straight line. The exchange contribution to the pressure becomes less negative due to relativity and turns positive in the extreme relativistic region. This was expected since it was already clear from the work of MacDonald and Vosko[10] that the exchange energy density itself changes sign in the ultrarelativistic limit. This is due solely to the transverse component of the exchange energy density.

This obviously implies that over a large range of pressures, exchange is considerably less important in the relativistic case. However, once the relativistic exchange pressure $p_{x\alpha}$ has turned positive, the ratio with respect to the relativistic kinetic pressure was found to level off to a constant. This behavior is, of course, remarkably different from the nonrelativistic case where everything becomes kinetic at high enough densities. Analysis of the asymptotic behavior of $\epsilon_{x\alpha}$ yields a power-law behavior similar to the kinetic case

$$\epsilon_{x\alpha} \underset{\rho_0\to\infty}{=} -\frac{1}{2}\varepsilon_x = \frac{3}{8}\left(\frac{3}{\pi}\right)^{1/3} e^2\rho_0^{4/3}, \tag{22}$$

which implies an asymptotic contribution to the pressure given by

$$p_{x\alpha} \underset{\rho_0\to\infty}{=} \frac{1}{8}\left(\frac{3}{\pi}\right)^{1/3} e^2\rho_0^{4/3}. \tag{23}$$

The asymptotic ratio of the relativistic exchange pressure to the kinetic pressure in the limit of very high compressions then immediately follows from these results to be

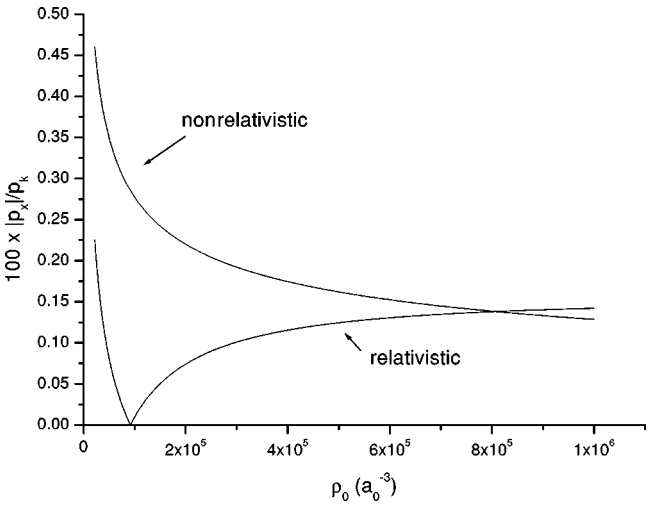

FIG. 4. Percentage ratio of the (absolute value of the) exchange contribution to the pressure $|p_x|$ to the kinetic contribution p_k, both for the nonrelativistic and the relativistic cases. The importance of exchange is seen to decay much more rapidly in the relativistic case, but it levels off to a constant nondiminishing fraction of the kinetic contribution after turning positive in the ultrarelativistic limit.

$$\frac{p_{x\alpha}}{p_{k\alpha}} \underset{\rho_0\to\infty}{=} \frac{1}{2\pi}\alpha \tag{24}$$

with α the fine-structure constant as defined above. Evidently for $\alpha=0$ we recover the nonrelativistic result. The percentage ratio of the absolute value of the exchange contribution to the pressure $p_{x\alpha}$ to the kinetic contribution $p_{k\alpha}$ is plotted in Fig. 4.

3. Total relativistic pressure

Figure 5 shows the total relativistic correction percentage as a function of electron density ρ_0. A useful parameter to

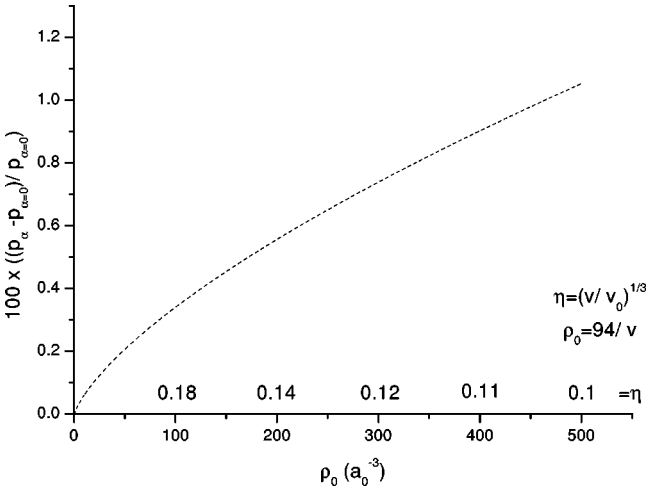

FIG. 5. Total relativistic percentage correction versus density. Corresponding values for compression parameter η for Pu are also shown, assuming the electrons in Pu form a nonresponsive uniform electron gas. The value for v_0 was taken from Table I.

TABLE I. Experimental data for the equilibrium volume v_0, bulk moduli K_0, and the pressure derivative of the bulk modulae K_1 for Ta and Pu. Thermodynamic data on Ta taken from Ref. 25. Thermodynamic data for Pu taken from Ref. 26 (V_0) and Ref. 27 (K_0 and K_1).

	Ta	Pu
V_0 (a.u.)	121.75	168
K_0 (Mbar)	1.95	0.42
K_1	3.4	10.5

understand the physics involved in the range of densities depicted is the compression parameter η defined as

$$\eta=(v/v_0)^{1/3} \tag{25}$$

with v here denoting the atomic volume and v_0 its value at normal conditions. Focusing, for instance, on Pu, and assuming all electrons form a nonresponsive background for the nuclei, i.e., $\rho_0=94/v$, one already requires roughly a compression of the volume by a factor 10^3 (i.e., $\eta=0.1$) to reach a modest relativistic correction of 1%. The value for v_0 taken for Pu is listed in Table I, together with some other relevant experimental data for Ta and Pu used in this work.

III. OBTAINING BOUNDARY DENSITIES FROM RELATIVISTIC THOMAS-FERMI THEORY

A. Vallarta-Rosen theory

1. Formulas

The Vallarta-Rosen (VR) theory was the first relativistic TF theory proposed. Its derivation is intuitive and consists in essence of solving the relativistic local Euler equation which expresses the fact that the total energy of the fastest electron is a constant throughout the electron cloud in the solid

$$\mu_\alpha=\frac{\partial t_\alpha}{\partial n}+V(\mathbf{r}) \tag{26}$$

with $\partial t_\alpha/\partial n$ given by Eq. (11), simultaneously with Poisson's equation

$$\nabla^2 V=-4\pi e^2\rho+4\pi Ze^2\rho_{ext}, \tag{27}$$

where $Ze\rho_{ext}$ denotes the external core charge, assumed normalized to the atomic number Z. Assuming ρ_{ext} to be spherically symmetric the problem becomes one dimensional in the radius r, and making the substitution for the screening function $\phi(x)$

$$[\mu-V(r)]=\frac{Ze^2}{r}\phi(x) \tag{28}$$

with

$$r=b_{VR}x, \quad b_{VR}=\frac{1}{4}\left[\frac{9\pi^2}{2Z}\right]^{1/3}a_0,$$

one then obtains the relativistic generalization of the dimensionless TF equation $d^2\phi(x)/dx^2=\phi^{3/2}/x^{1/2}$, namely,

$$\frac{d^2}{dx^2}\phi(x)=\frac{\phi^{3/2}}{x^{1/2}}\left[1+\lambda\left(\frac{\phi}{x}\right)\right]^{3/2}-4\pi x b_{vr}^3\rho_{ext}(bx) \tag{29}$$

with

$$\lambda=\left(\frac{4}{3\pi}\right)^{2/3}\alpha^2 Z^{4/3}. \tag{30}$$

Within the above framework the radial number density is then obtained as

$$\rho(r)d\mathbf{r}=Zx^{1/2}\phi^{3/2}\left[1+\lambda\left(\frac{\phi}{x}\right)\right]^{3/2}dx. \tag{31}$$

2. Short discussion

In essence the TF limit in DFT can be justified by assuming that the potential varies slowly compared to the wavelength of electrons on the Fermi surface. In the nonrelativistic case imposing this condition on the exact energy expressions allows one to derive the TF theory from first-principles theory.[17]

No such derivation has been given as yet for the full VR theory and given the problem of the non-normalizable divergent density at the origin when one makes the assumption

$$\rho_{ext}(r)=\delta(0) \tag{32}$$

already discussed in the introduction, various different forms for relativistic TF theory have thus far been presented.[18] We wish to emphasize strongly, however, that the linearized form of the VR theory has been obtained from first-principles theory in the work of Baltin and March[19] on the linear response of a relativistic electron gas. To the knowledge of the authors at the time of writing, no other form of relativistic TF theory can make a similar claim concerning its full and/or asymptotic validity.

B. Solving the Vallarta-Rosen equation

1. Choice of the nuclear profile

We will proceed to solve the equation for the self-consistent potential V. To obtain a normalizable density we take into account the finite extension of the nucleus. If one describes the core charge by a Fermi-Dirac distribution function, the radius for which the charge drops to half of its maximum value is obtained from experiment to be[20]

$$r_c=1.07A^{1/3}10^{-15}m \tag{33}$$

with A the atomic mass. Following Hill *et al.*[21] we approximated the nucleus by a homogeneously charged sphere and the relation (33) was used to obtain an estimate for the radius. This then yields as an explicit expression for the nuclear charge profile

$$\rho_{ext}(r)=\frac{1}{\frac{4}{3}\pi r_c^3}\Theta(r_c-r)$$

with $\Theta(r_c-r)$ the Heaviside step function. The term to be added to the right-hand side of the VR equation then reads

$$4\pi x b_{vr}^3 \rho_{ext}(bx) = 3\Theta(x_c-x)\frac{x}{x_c^3}.$$

2. Reduction to an equivalent set of first-order equations

The second-order Vallarta-Rosen Eq. (29) was split up into two first-order differential equations

$$\frac{d\phi(x)}{dx} = y(x), \tag{34}$$

$$\frac{dy(x)}{dx} = \frac{\phi^{3/2}}{x^{1/2}}\left[1+\lambda\left(\frac{\phi}{x}\right)\right]^{3/2} - 3\Theta(x_c-x)\frac{x}{x_c^3}, \tag{35}$$

which were solved simultaneously using the numerical Fehlberg fourth–fifth-order Runge-Kutta method. Since the right-hand side of the second differential Eq. (35) diverges as x tends to zero, one must use a small-x expansion to get away from the origin. As discussed below, this expansion is fully determined by the normalization condition and the specific form of the nuclear charge distribution ρ_{ext}.

3. Boundary conditions

a. At the origin. Starting from Poisson's Eq. (27), one immediately obtains after integration

$$\int_0^R 4\pi r^2 \rho dr = Z\left\{\lim_{x\to 0}\left[\phi(x) - x\frac{d\phi}{dx}(x)\right]\right\} + Z \tag{36}$$

and so in order to obtain a normalized solution ($\int_0^R 4\pi r^2\rho dr = Z$) for the VR equation it is sufficient that one has a solution satisfying

$$\lim_{x\to 0}\left[\phi(x) - x\frac{d\phi}{dx}(x)\right] = 0, \tag{37}$$

which implies that the self-consistent field must have an extremum at the center of the WS sphere

$$\left.\frac{dV}{dr}\right|_{r\to 0} = 0. \tag{38}$$

For comparison, note that for the classical TF equation, one only takes account of the Dirac-delta core through the boundary condition and so the normalization condition becomes

$$\lim_{x\to 0}\left[\phi(x) - x\frac{d\phi}{dx}(x)\right] = 1, \tag{39}$$

which is fulfilled by the small x expansion of Baker.[22]

b. At small x. At small x, the VR Eq. (29) with a homogeneously charged core reduces to

$$\partial_x^2\phi = \lambda^{3/2}\frac{\phi^3}{x^2} - 3\Theta(x_c-x)\frac{x}{x_c^3}. \tag{40}$$

Since a normalized solution of the VR equation $\phi(x)$ goes to zero at the origin faster than $x^{2/3}$, a valid small-x expansion must satisfy

$$\partial_x^2\phi = -3\frac{x}{x_c^3} \tag{41}$$

and a solution of this equation which satisfies the condition (37) is given by

$$\phi(x) = \frac{1}{2}\frac{x}{x_c}\left[3-\left(\frac{x}{x_c}\right)^2\right]. \tag{42}$$

In order to bring in the remaining integration constant b we considered the small-x expansion

$$\phi(x) = \frac{1}{2}\frac{x}{x_c}\left[3-\left(\frac{x}{x_c}\right)^2\right] + bx + \ldots \tag{43}$$

as was already obtained by Hill *et al.*[21] Both for the VR equation and the TF equation with a core this solution was used up to an arbitrary small value for x taken to be 0.01 times the nuclear radius.

c. At the WS-sphere. In terms of the screening function $\phi(x)$ the boundary condition at the WS sphere with dimensionless radius X becomes

$$\phi(X) - X\frac{d\phi}{dx}(X) = 0. \tag{44}$$

One cannot from the outset solve Eq. (29) for a given X due to the complexity of the boundary condition (44): one varies instead the independent integration constant b, and the corresponding X of the solution is then found for a given value for b as the zero of the function $\phi(x) - x\,d\phi/dx\,(x)$. Given the expected smallness of the relativistic correction it is of crucial importance that we compare relativistic and nonrelativistic boundary densities at exactly the same value for X. We therefore did not rely on previously obtained results for the nonrelativistic TF theory by Slater and Krutter[4] or Feynman *et al.*[5] but instead solved the nonrelativistic TF equation again for the same set of X values as used for the relativistic VR equation. Interpolation of the nonrelativistic solution to different X values yielded, however, perfect agreement with the results from earlier work. For the nonrelativistic TF equation, which needs to be solved only once for a given X since its solution in terms of $\phi(x)$ is independent of the element considered, we used Baker's expansion[22] up to the ninth term.

IV. NUMERICAL RESULTS: EOS FROM RELATIVISTIC TF THEORY FOR TA AND PU

A. Relativistic corrections to the TF density profile

1. Facts

Table II lists the values obtained for the nonrelativistic screening function $\phi(X)$ from nonrelativistic TF theory together with the values for the integration parameter, termed b here in analogy with the expansion (43), of Baker's[22] expan-

TABLE II. Solution $\phi(x)$ of the classical Thomas-Fermi equation evaluated at the dimensionless boundary of the WS cell X. b is the integration constant in Baker's small-x expansion (Ref. 22). The numbers in parentheses denote the uncertainty in the last digit(s).

X	b	$\phi(X)$
1.0000(1)	−0.63870000	1.77878(18)
2.0000(1)	−1.46725000	0.75652(4)
3.0000(1)	−1.55847000	0.431515(14)
4.0000(1)	−1.57829750	0.279347(7)
5.0000(1)	−1.58420800	0.194684(4)
6.0000(1)	−1.58634380	0.1425562(24)
7.0000(1)	−1.58722485	0.1082322(15)
8.0000(1)	−1.58762600	0.0844921(10)
9.0000(1)	−1.58782325	0.067441(7)
10.000(1)	−1.58792645	0.054819(5)
11.000(1)	−1.58798325	0.045252(4)
12.000(1)	−1.58801590	0.037848(3)
13.000(1)	−1.58803540	0.0320050(25)
14.000(1)	−1.58804740	0.027337(19)
15.000(1)	−1.58805500	0.0235571(16)

sion. Tables III and IV list solutions for $\phi(X)$ for Ta and Pu, respectively, from VR theory together with the corresponding values for the integration constant b appearing in the small-x expansion (43). All relevant properties can be calculated from the data presented in these tables.

From Eq. (31), which encompasses the nonrelativistic result for $\lambda=0$, one can then immediately obtain the corresponding values for the boundary density both in the nonrelativistic (TF without core) case, say, denoted by $\rho_{nr}(R)$, and in the relativistic case, say, $\rho_r(R)$. The difference between both densities is plotted in Fig. 6(a) and Fig. 6(b) for Ta and Pu, respectively, as a function of the compression parameter η. The boundary density was, for all compressions considered, found to be lowered by relativity.

2. Discussion: Effect of the finite nucleus

To examine the effect of a finite nucleus on the boundary density $\rho(R)$ we have switched off the fine-structure constant α in the VR calculations for Ta (with a finite-size nucleus) and compared the resulting charge-density profile, say, $\rho_{nr}^{c}(r)$, with that from the classical TF calculation $\rho_{nr}(r)$ for an arbitrarily chosen value $X=7$. Both density profiles are plotted in Fig. 7(a). The difference is seen to manifest itself mainly very close to the origin.

TABLE III. Solution $\phi(x)$ of the Vallarta-Rosen equation for Ta evaluated at the dimensionless boundary of the WS cell X. b is the integration constant in the small-x expansion (43). The numbers in parentheses denote the uncertainty in the last digit(s).

X	b	$\phi(X)$
1.0000(1)	−4.415	1.72825(17)
2.0000(1)	−5.1822	0.74596(4)
3.0000(1)	−5.268458	0.426851(14)
4.0000(1)	−5.2873138	0.276719(7)
5.0000(1)	−5.292954	0.193018(4)
6.000(1)	−5.2949936	0.141387(24)
7.000(1)	−5.295865	0.107419(15)
8.000(1)	−5.2962491	0.083906(10)
9.000(1)	−5.2964385	0.066986(7)
10.000(1)	−5.29653766	0.054452(5)

TABLE IV. Same as Table III, but for Pu.

X	b	$\phi(X)$
1.0000(1)	−5.749	1.70877(17)
2.0000(1)	−6.4921	0.74171(4)
3.0000(1)	−6.576331	0.424914(14)
4.0000(1)	−6.5947815	0.275640(7)
5.0000(1)	−6.6003054	0.192326(4)
6.0000(1)	−6.6023068	0.1409593(23)
7.000(1)	−6.60313444	0.1071036(23)
8.00(1)	−6.603512151	0.083636(10)
9.000(1)	−6.603698	0.066796(10)
10.000(1)	−6.603795	0.054345(10)

Contrary to the nonrelativistic case, the relativistic density profile was found to exhibit a significant charge pileup immediately outside the nucleus. The height, width, and position of this pileup were each found to depend strongly on the chosen value for the radius. For comparison, Fig. 7(b) shows the charge profile for Ta for $X=7$ both for the original core radius x_c, and for a core taken to be 1.5 times x_c. A large charge difference manifests itself very near to the nucleus and this is consequently compensated by a very small difference in charge, the two curves lying within graphical accuracy almost on top of one another, over most of the WS sphere. The difference in density at the boundary because of the different radius was finally (even for the highest compression we considered, $X=1$) found to be of the order of 1/50 of the difference due to relativity. This is shown in Fig. 7(c) for Ta. We conclude that the equation of state, within the present scheme, is barely affected by (reasonable) different choices concerning the size of the nucleus. One must, however, be careful when using the charge-density profile to calculate other properties such as the energy. Similar results were obtained for the case of Pu.

B. EOS for Ta and Pu

We now use the values for $\rho_{nr}(R)$ and $\rho_r(R)$ to calculate the nonrelativistic and relativistic EOS from Eq. (6) for $\alpha=0$ and $\alpha=1/137$, respectively. We note from the discussions presented above that the relativistic effects both at the level of the EOS of the uniform electron gas, and at the level of the boundary electron density $\rho(R)$, work "in the same direction:" both lead to a lowering of the pressure compared to the nonrelativistic case.

1. Tantalum

a. Results plus comparison with other calculations. Figure 8(a) plots the results obtained from our work for Ta compared with the results from Boettger.[1] Clearly for low pres-

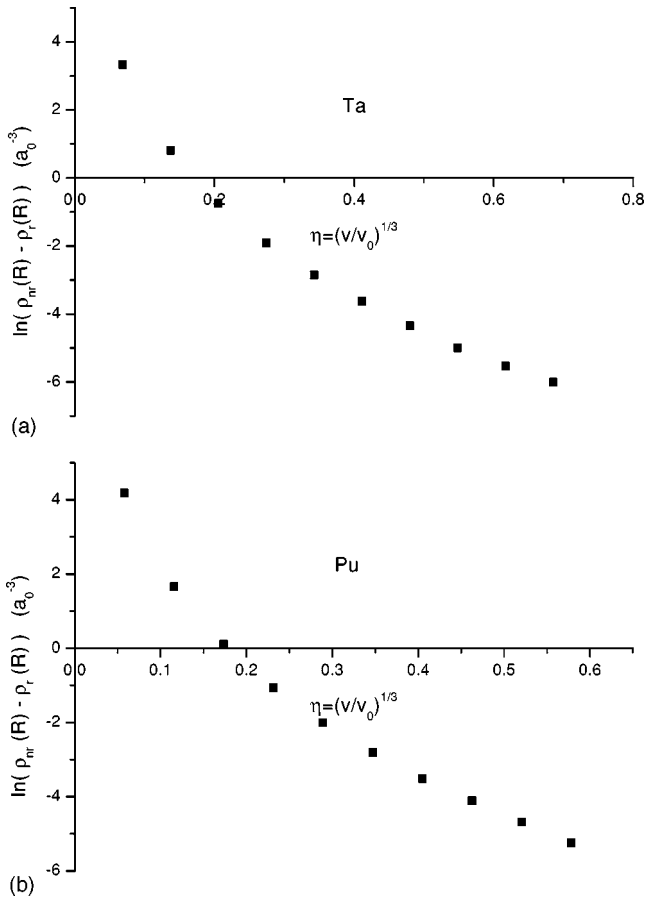

FIG. 6. (a) Difference in boundary electron density from classical TF theory (ρ_{nr}) and VR theory (ρ_r) for Ta versus compression ratio η. For clarity of presentation, the logarithm of the values in a.u. was taken. (b) Same as for (a), but for Pu.

sures, the method we have used is not quantitative. However both curves approach one another quickly with increasing pressure and the results of Boettger seem to lead, quite naturally, into the region where the EOS can be determined adequately by the relativistic TF theory. A detailed plot exposing the relativistic correction to the results from nonrelativistic TF theory is given in Fig. 8(b). As already discussed earlier, the total correction to the pressure is negative.

b. Comparison with analytic EOS. Since Ta has no known structural phase transitions under pressure, we expect our results to coincide at high compressions with predictions from analytic parametric EOS, which make use of equilibrium values for the bulk modulus and its derivatives. The most advanced expressions, nonrelativistic, however, describing the very high-pressure regime are given by Holzapfel,[23] and we will make specifically use of the so-called *APL* form, where L denotes an index. The expression for the pressure is then given in terms of the compression parameter η by

$$P = 3K_0 \eta^{-5}(1-\eta)e^{[c_0(1-\eta)]}\left[1+\eta\sum_{k=2}^{L} c_k(1-\eta)^{k-1}\right], \tag{45}$$

where K_0 denotes the bulk modulus at equilibrium and $c_0 = -\ln(3K_0/p_{k\alpha=0})$. If we write the derivative of K_0 with respect to pressure as K_1 we immediately obtain from Eq. (45) that

$$c_2 = \frac{3}{2}(K_1 - 3) - c_0. \tag{46}$$

For our purposes, the *APL* EOS with $L=2$, which requires experimental input values only for K_0 and K_1, will suffice. The values for Ta are taken from Table I. The resulting curve is plotted together with the numerical results of this work and those of Boettger also in Fig. 8(a).

The $AP2$ equation of state is seen to describe the low-pressure results of Boettger very well. However, for the higher-pressure values, the $AP2$ equation of state underestimates the predictions from Boettger's calculations. To illustrate this further, Fig. 8(c) plots the difference between the $AP2$ predictions and Boettger's results as a function of volume. Whereas for compressions $\eta \gtrsim 0.9$ both results are clearly in good agreement, the difference oscillating weakly around zero, they are seen to diverge quickly for higher compressions, say, $\eta < 0.9$.

Because of this, the clear tendency of Boettger's results to approach the results from our work, as noted already above, is less present in the analytic form $AP2$: the $AP2$ equation of state stays on the contrary nearly parallel to our results on a logarithmic plot over a broad pressure range and only tends towards our results in the extreme compression regime. Of course, at compressions where the uniform electron-gas limit is reached, the $AP2$ form will yield the nonrelativistic $\rho^{5/3}$ behavior, whereas our pressure results will be proportional to $\rho^{4/3}$. Various other analytic EOS, using, however, the same input variables, gave rise to similar conclusions.

From the above discussion, however, it seems fair to expect our results to become quantitative well before the extreme compression regime as suggested by the comparison with $AP2$. Further wave-mechanical calculations to confirm this point would clearly be of interest.

2. Plutonium

a. Results plus comparison with other calculations. Figure 9(a) plots the results obtained from our work for the EOS of Pu. To the authors' knowledge at the time of writing, no results from wave-mechanical calculations on the high-pressure EOS have up to now been published, and so a direct comparison, as for Ta, did not prove possible.

b. Comparison with analytic EOS. Contrary to Ta, Pu is expected to undergo at least one phase transition with increasing pressure.[9] We therefore do not expect any analytic EOS using equilibrium data as input to tend towards our limiting predictions from TF theory before both reach the free-electron-gas limit. The $AP2$ result is also plotted in Fig. 9(a). Input values for Pu were taken from Table I. Surprisingly the analytic equation of state was found not to differ too strongly from our numerical results, compared, for instance, with the results for Ta. Of course, close to the uniform electron-gas limit, all EOS become independent of the chosen values for the parameters for bulk modulus, its de-

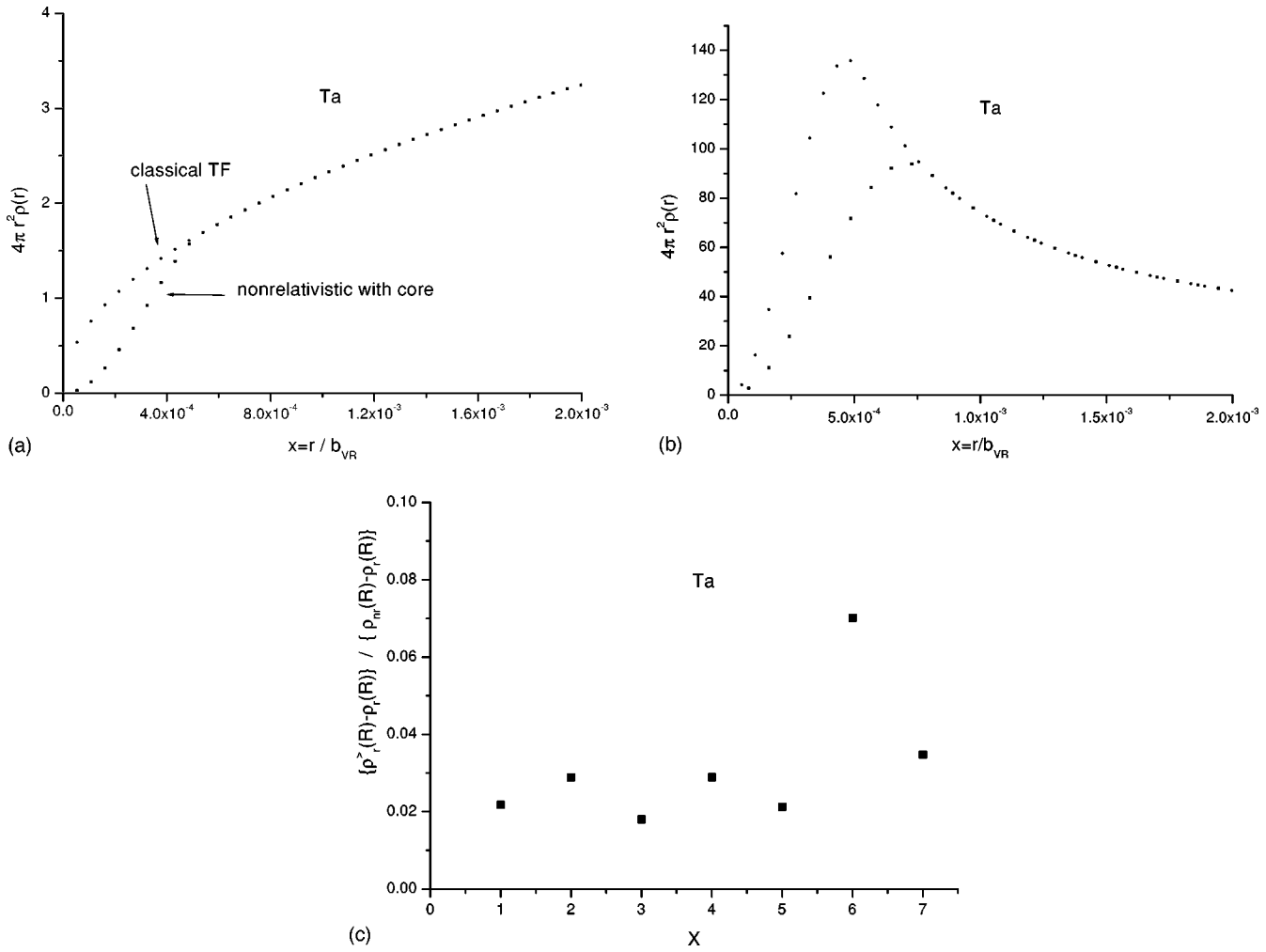

FIG. 7. (a) Radial electron-density profile for Ta for $X=7$ from nonrelativistic TF theory with (ρ^c_{nr}) and without (ρ_{nr}) a finite nucleus. Profile is only shown very close to the origin of the WS sphere, where the difference is mainly manifested. (b) Radial electron-density profile for Ta from VR theory for two different values of the nuclear radius, r_c, as calculated from Eq. (33) and 1.5 times r_c. (c) Difference between the relativistic density at the boundary R of the WS sphere using the original core size r_c as derived from Eq. (33) [denoted by $\rho_r(R)$] and that using a core of radius $1.5\times r_c$ [denoted by $\rho^{>}_r(R)$] as a fraction of the difference due to relativity given by $\{\rho_{nr}(R)-\rho_r(R)\}$. The results are given for different values of the dimensionless WS radius X. Reasonably different choices for the core size are seen to lead, even for the highest compression $X=1$, to only very small corrections (of the order of 2%) compared to the correction due to relativity itself.

rivatives, and the equilibrium volume, and they depend only on Z.

Figure 9(b) plots the relativistic corrections to the pressure for Pu over a broad range of pressures. The magnitude of the corrections was found to depend only very slightly on the change in Z from 73 to 94.

V. FUTURE DIRECTIONS

It would be of clear interest if further wave-mechanical calculations could be performed to determine more precisely the range of pressures where the relativistic TF method becomes quantitative. Possible improvements of the work presented here are to include exchange into relativistic TF theory. When solving for the potential it has not proven possible to solve the Euler equation including exchange for the density in terms of the potential $V(r)$, which is obviously a necessary prerequisite to obtain a single differential equation for $V(r)$ from Poisson's equation. However, one can equally well solve immediately for the density, and within this route a single differential equation for the density which takes exchange into account can be written down.[24]

Finally, our attention was drawn to the work of Engel and Dreizler[29] in which low-order gradient corrections are introduced into relativistic TF theory paralleling the nonrelativistic approach of von Weizsäcker.[30] This would afford an alternative approach to the problem in the original Vallarta-Rosen theory that the electron density is not normalizable because of the enhanced singularity of $\rho(r)$ at a point nucleus beyond the (normalizable) $r^{-3/2}$ divergence in the nonrelativistic TF limit. While that problem has been bypassed here by adopting a nonzero nuclear radius, it would be of interest in the future to compare and contrast the Engel and Dreizler approach with the present one. This would also allow direct calculations of ground-state energies, whereas

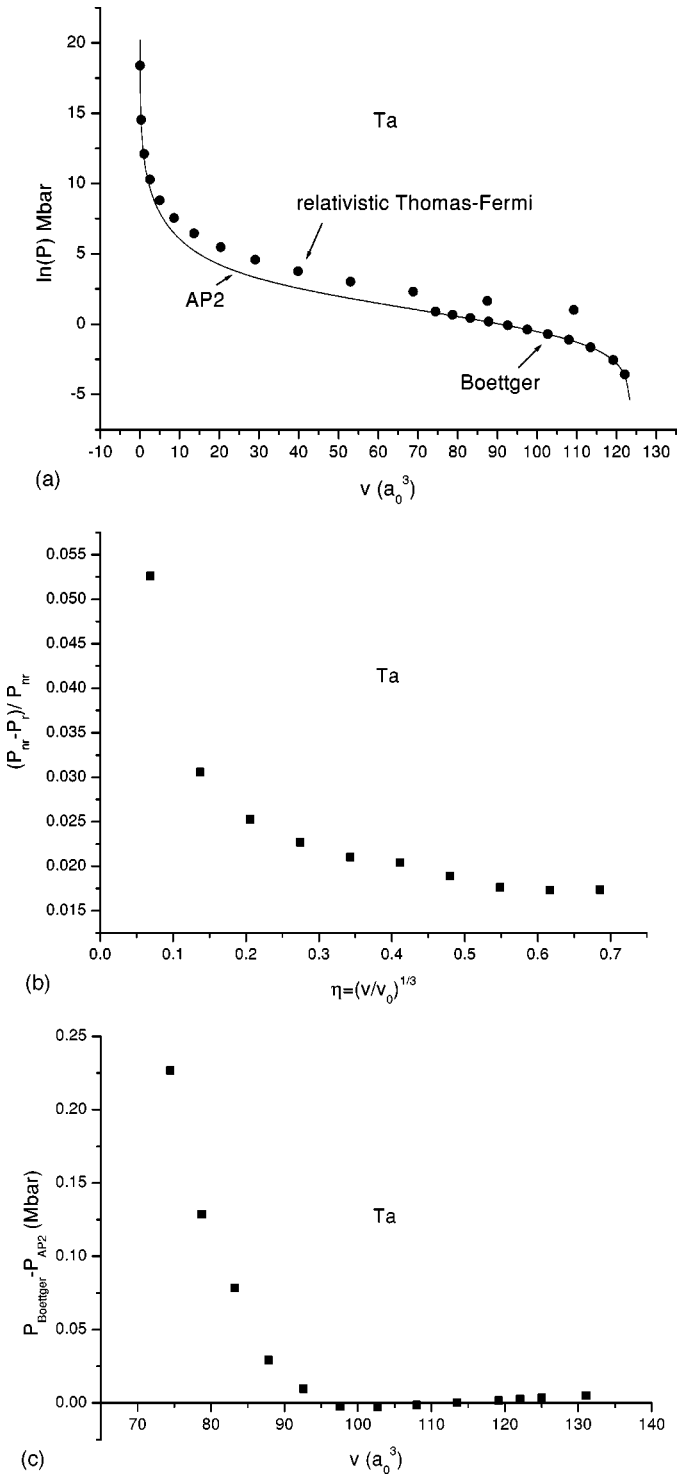

FIG. 8. (a) EOS for Ta from relativistic VR theory (this work) and from Dirac's equation (Boettger, Ref. 1). The solid curve shows the analytic $AP2$ equation of state of Holzapfel, Ref. 23 using the experimental data of Table I as input for the parameters. (b) Difference in pressure for Ta between nonrelativistic P_{nr} and relativistic treatments P_r within fully local DFT versus the compression parameter η. (c) Difference in pressure for Ta between the numerical results of Boettger, Ref. 1, and the predictions from the analytic equation of state $AP2$ of Holzapfel, Ref. 23.

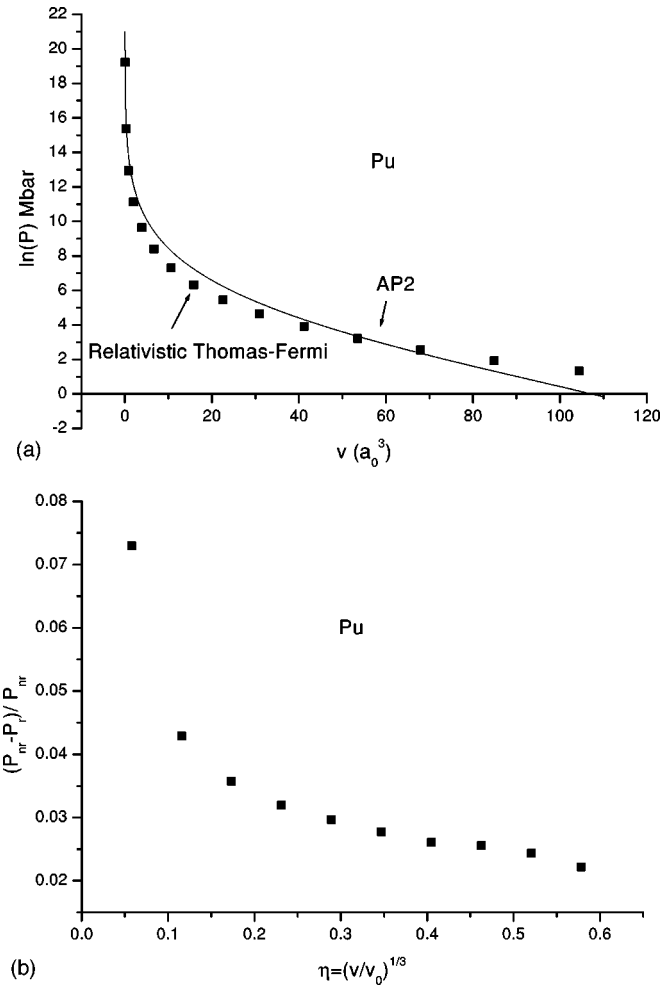

FIG. 9. (a) EOS for Pu from relativistic VR theory (this work). The solid curve shows the analytic $AP2$ equation of state of Holzapfel, Ref. 23, using the experimental data of Table I as input for the parameters. (b) Difference in pressure for Pu between nonrelativistic P_{nr} and relativistic treatments P_r within fully local DFT versus the compression parameter η.

the entire focus of our finite nucleus radius treatment has, of course, been on the equations of state.

ACKNOWLEDGMENTS

The authors would like to thank Dr. J. C. Boettger for supplying us with a preprint of Ref. 1, and Dr. G. Straub for his continuing interest and support. It is also our pleasure to thank Professor W. B. Holzapfel for useful and stimulating discussions.

APPENDIX A: THE ROLE OF THE VIRIAL IN COMPLETELY LOCAL RELATIVISTIC DFT

1. Introduction

In earlier work by one of us,[28] explicit relations were established revealing the role of the virial in completely local relativistic DFT. The theory was written down for heavy atoms and the aim of this Appendix is to generalize these

results to the case of infinite systems with periodic boundary conditions as considered above within the spherical WS approximation.

2. Results

We start from the Euler equation given generally for a completely local theory by Eq. (26). For simplicity, we will leave out the index α when denoting the kinetic-energy density t.

Writing down the total kinetic energy and applying integration by parts yield

$$T=4\pi\int_0^R tr^2dr \tag{A1}$$

$$=\frac{4\pi}{3}t[\rho(r)]r^3|_0^R-\frac{4\pi}{3}\int_0^R\frac{dt}{dr}r^3dr. \tag{A2}$$

Let's now examine the behavior of the first term in the origin. In the VR theory the density is given by Eq. (31). In the nonrelativistic case ($\lambda=0$) ϕ goes to 1 as r tends to zero and so

$$\rho(r)\underset{r\geqslant 0}{\sim}\frac{1}{r^{3/2}}. \tag{A3}$$

Since the ''classical'' kinetic-energy density $t_0(\rho)$ is given by

$$t_0(\rho)=c_k\rho_0^{5/3}, \tag{A4}$$

it is clear that the first term of Eq. (A2) tends to zero as $\sqrt{r}$. In the relativistic case, with a point nucleus (so $\phi\geqslant 1$ *as* $r\geqslant 0$) the density already diverges as $1/r^3$ and inserting this into the relativistic kinetic-energy density will lead to a divergence of the term $t[\rho(r)]r^3$ at the origin in between $1/r^2$ (corresponding to $t\sim\rho_0^{5/3}$) and $1/r$ (corresponding to $t\sim\rho_0^{4/3}$). From the small-x expansion (43) it follows straightforwardly that this divergency in the origin is removed in the presence of a finite-size nucleus, $t[\rho(r)]r^3$ tending to zero in the origin, and so we conclude that

$$\frac{4\pi}{3}t[\rho(r)]r^3|_0^R=vt[\rho(R)] \tag{A5}$$

with v now the atomic volume.

Following March[28] we put, in the second term on the right of Eq. (A2),

$$\frac{dt}{dr}=\frac{dt}{d\rho}\frac{d\rho}{dr}=[\mu-V(r)]\frac{d\rho}{dr} \tag{A6}$$

and integrating again by parts gives, for the second term,

$$\begin{aligned}-\frac{4\pi}{3}\int_0^R[\mu-V(r)]\frac{d\rho}{dr}r^3dr&\\ =-\frac{4\pi}{3}[\mu-V(r)]r^3\rho|_0^R+\frac{4\pi}{3}\int_0^R\rho\mu 3r^2dr&\\ -\frac{4\pi}{3}\int_0^R\rho V3r^2dr-\frac{4\pi}{3}\int_0^R\rho r\frac{dV}{dr}r^2dr&\\ =-\frac{4\pi}{3}[\mu-V(r)]r^3\rho|_0^R+N\mu-\int\rho Vd\mathbf{r}+\frac{1}{3}\langle\mathbf{r}\cdot\mathbf{F}\rangle,&\end{aligned} \tag{A7}$$

where we define $\mathbf{F}$ in the usual manner as $-\nabla V$. Evaluation of the first term on the right in the origin again depends on the use of a core. If present, it evaluates to zero in the origin and so

$$\begin{aligned}-\frac{4\pi}{3}[\mu-V(r)]r^3\rho|_0^R&=-v[\mu-V(R)]\rho(R)\\ &=-v\frac{dt}{d\rho}[\rho(R)]\rho(R).\end{aligned} \tag{A8}$$

Combining the above equations now gives

$$\langle T\rangle=-v\left[\rho\frac{dt}{d\rho}-t\right]_R+N\mu-\int\rho Vd\mathbf{r}+\frac{1}{3}\langle\mathbf{r}\cdot\mathbf{F}\rangle, \tag{A9}$$

which is the central result of this Appendix.

We now use the Euler equation to eliminate the chemical potential μ. Multiplying the Euler equation throughout by the density ρ and integrating over the WS cell gives

$$N\mu=\int\rho\frac{dt}{d\rho}d\mathbf{r}+\int\rho Vd\mathbf{r}. \tag{A10}$$

Inserting this into Eq. (A9) gives

$$\langle T\rangle=-v\left[\rho\frac{dt}{d\rho}-t\right]_R+\int\rho\frac{dt}{d\rho}d\mathbf{r}+\frac{1}{3}\langle\mathbf{r}\cdot\mathbf{F}\rangle. \tag{A11}$$

Again following March[28] by differentiating the Euler equation with respect to r, also the virial of the force can be reformulated in terms of the kinetic energy, giving

$$\langle\mathbf{r}\cdot\mathbf{F}\rangle=\int\rho r\frac{d}{dr}\left[\frac{dt}{d\rho}\right]d\mathbf{r} \tag{A12}$$

and so

$$\langle T\rangle=-v\left[\rho\frac{dt}{d\rho}-t\right]_R+\int\rho\frac{dt}{d\rho}d\mathbf{r}+\frac{1}{3}\int\rho r\frac{d}{dr}\left[\frac{dt}{d\rho}\right]d\mathbf{r}. \tag{A13}$$

The main merit of this procedure, avoiding the integration of the complicated expression for the relativistic kinetic-energy

density t_α when evaluating the contribution of the kinetic energy, is not lost since the evaluation of t_α is only at one particular density, namely, the boundary density. Remarkably, the contribution to the kinetic energy, because of the finite sphere radius, is negative and turns out to be (in magnitude) just the volume times the kinetic contribution to the pressure. Of course, the total kinetic energy will increase because of confinement but this increase will come from a higher value for the last two terms in the right-hand side of Eq. (A13).

[1] J.C. Boettger, Phys. Rev. B **64**, 035103 (2001).
[2] M.S. Vallarta and N. Rosen, Phys. Rev. **41**, 708 (1932).
[3] F.E. Leys, N.H. March, D. Lamoen, and V.E. Van Doren, High Press. Res. **22**, 217 (2002).
[4] J.C. Slater and H.M. Krutter, Phys. Rev. **47**, 559 (1935).
[5] R.P. Feynman, N. Metropolis, and E. Teller, Phys. Rev. **75**, 1561 (1949).
[6] L.H. Thomas, Proc. Cambridge Philos. Soc. **23**, 542 (1927).
[7] E. Fermi, Z. Phys. **48**, 73 (1928).
[8] E.P. Wigner and F. Seitz, Phys. Rev. **43**, 804 (1933).
[9] P. Sönderlind, O. Eriksson, B. Johansson, J.M. Wills, and A.M. Boring, Nature (London) **374**, 524 (1995).
[10] A.H. MacDonald and S.H. Vosko, J. Phys. C **12**, 2977 (1979).
[11] H. Jensen, Z. Phys. **82**, 794 (1933); J. Ferreirinho, R. Ruffini, and L. Stella, Phys. Lett. **91B**, 314 (1980).
[12] See, for instance, S. Lundqvist and N. H. March, *Theory of the Inhomogeneous Electron Gas* (Plenum, New York, 1983).
[13] R. Baltin and N.H. March, J. Phys. A **20**, 5517 (1987).
[14] S.D. Kenny, G. Rajagopal, R.J. Needs, W.-K. Leung, M.J. Godfrey, A.J. Williamson, and W.M.C. Foulkes, Phys. Rev. Lett. **77**, 1099 (1996).
[15] See, e.g., W. Jones and N. H. March, *Theoretical Solid State Physics* (Dover, New York, 1985).
[16] L. D. Landau and E. M. Lifshitz, *Statistical Physics* (Pergamon, London, 1959).
[17] N. H. March, W. Young, and S. Sampanthar, *The Many Body Problem in Quantum Mechanics* (Dover, New York, 1995).
[18] See, e.g., N. H. March, *Self-Consistent Field in Atoms and Molecules* (Pergamon, NY, 1975); Y.C. Leung and Shou-Yong Pei, Phys. Rev. A **40**, 2731 (1989).
[19] R. Baltin and N.H. March, Phys. Rev. A **37**, 3942 (1988). See also F. E. Leys, N. H. March, G. G. N. Angillela, and D. Lamoen (unpublished).
[20] H. Semat and J. R. Albright, *Introduction to Atomic and Nuclear Physics* (Chapman and Hall, London, 1972), p. 579.
[21] S.H. Hill, P.J. Grout, and N.H. March, J. Phys. B **17**, 4819 (1984).
[22] E.B. Baker, Phys. Rev. **36**, 630 (1930)
[23] See, e.g., W.B. Holzapfel, High Press. Res. **16**, 81 (1998).
[24] N.H. March, Int. J. Quantum Chem. **70**, 779 (1998).
[25] H. Cynn and C.S. Yoo, Phys. Rev. B **59**, 8526 (1999).
[26] J. Donohue, *The Structure of the Elements* (Krieger, Malabar, Florida, 1982).
[27] R. B. Roof, in *Compression and Compressibility Studies of Plutonium and a Plutonium-Gallium Alloy*, edited by D. K. Smith, C. Barret, D. E. Leyden, and P. K. Predecki (Plenum, New York, 1981), Vol. 24, p. 221.
[28] N.H. March, Phys. Rev. A **48**, 4778 (1993).
[29] E. Engel and R.M. Dreizler, Phys. Rev. A **38**, 3909 (1988).
[30] C.F. von Weizsäcker, Z. Phys. **96**, 431 (1935).